J Water Environ Nanotechnol 2026, 11(3): 311-325
10.22090/jwent.2025.2076875.2001

RESEARCH PAPER

Incorporation of Silver-Decorated Graphene Oxide Into PSf Nanocomposite Membrane to Be Used in MBR System

Samaneh Kazemi[1], Soroush Khakpour[2], Yoones Jafarzadeh[1*], Reza Yegani[1,3]

[1] Faculty of Chemical Engineering, Sahand University of Technology, Tabriz, Iran
[2] Department of Civil Engineering and Architecture (DICAR), University of Catania, via Santa Sofia 64, Catania, Italy
[3] Membrane Technology Research Centre, Sahand University of Technology, Tabriz, Iran

*Corresponding Author(s)
Email:
yjafarzadeh@sut.ac.ir

Article History:

Received: 2025-11-05
Revised: 2026-01-20
Accepted: 2026-01-30

How to cite this article
Kazemi S, Khakpour S, Jafarzadeh Y, Yegani R. Incorporation of Silver-decorated Graphene Oxide into PSf Nanocomposite Membrane to be Used in MBR System. J Water Environ Nanotechnol 2026, 11(3): 311-325, DOI: 10.22090/jwent.2025.2076875.2001

HIGHLIGHTS

- GO-Ag incorporation enhanced PSf membrane hydrophilicity, flux, and mechanical strength.
- Ag anchoring on GO nanosheets suppressed silver release from the membrane matrix.
- GO-Ag membranes showed superior antibacterial and antifouling performance versus neat PSf.

ABSTRACT

The GO-Ag nanocomposite was synthesized and incorporated as hydrophilic and antibacterial nanoparticles into the PSf membrane. The X-ray diffraction (XRD) and ultraviolet (UV) analyses verified the successful synthesis of the GO-Ag nanocomposite, while the Field Emission Scanning Microscope (FESEM) and Energy Dispersive X-Ray (EDX) analyses revealed that Ag nanoparticles were evenly attached to Graphene Oxide (GO) nanosheets with little to no agglomeration. PSf polymeric membrane containing 0.1, 0.3, and 0.5 weight percent of GO-Ag nanoparticles. These nanoparticles were then characterized using a set of analyses, including FESEM, contact angle, pure water flow, abrasion resistance, tensile strength, elongation, and antibacterial test. The results showed that incorporating GO-Ag nanoparticles into PSf membranes enhanced the membranes' hydrophilicity, pure water flux, tensile strength, and abrasion resistance as the nanoparticle concentration rose in the polymeric matrix. The Inductively Coupled Plasma (ICP-OES) test was performed to determine the rate of Ag release from the membrane matrix, and the findings showed that embedding silver nanoparticles onto GO nanosheets considerably decreased Ag release. In addition, the introduction of GO-Ag nanoparticles improved the antibacterial properties of nanocomposite membranes, which were then used in a lab-scale MBR alongside the plain membrane. Nanocomposite membranes were found to have better antifouling properties than a neat PSf membrane.

KEYWORDS:

Polysulfone; Graphene oxide; Silver; Membrane bioreactor

©2026 The Author(s). Published by the Iranian Environmental Mutagen Society. This work is licensed under the Creative Commons Attribution 4.0 International License (CC BY 4.0). To view a copy of this license, visit http://creativecommons.org/licenses/by/4.0/.

1. INTRODUCTION

Membrane bioreactor (MBR) technology has attracted a lot of interest because of its exceptional qualities, which include its great efficiency in removing nutrients and its capacity to hold all biomass without requiring a subsequent clarifier. MBR systems, as opposed to traditional activated sludge processes, are more adaptable to a range of wastewater compositions and flow rate variations. Adapting traditional procedures to fluctuations in effluent properties and flow might be difficult at times. The implementation of MBR technology, which offers more operational flexibility and improved overall performance, thus constitutes a major advancement in wastewater treatment [1]. Membrane fouling has been a major obstacle to the widespread implementation of MBR systems, despite all their benefits. The clogging and fouling of membranes in MBRs are a complicated problem that is characterized by complex interactions among several components and has proven to be very challenging to regulate or precisely describe. This issue poses a significant obstacle to the further use of MBR technology in wastewater treatment applications as it lowers system efficiency and raises maintenance and operating expenses [1, 2]. Numerous consequences have been observed due to sediments: a decrease in both the flow of infuses and the function of the membrane, increased operational expenses, along with a decline in the lifetime of the membrane [3]. The potential for reducing biofouling in MBR systems has been studied in several works. The results of these studies fall into two major classes, according to the key mechanisms that lead to membrane fouling: a boost in the hydrophilicity of the membrane through combination with a hydrophile expletive or either moderating the surface of it [4, 5] and affixing antibacterial expletives to the membrane matrix, to enhance the antibacterial properties of the membrane [6, 7]. Protein-containing firm particles that are typically produced through the microorganism's metabolism were added to the membrane, to which the hydrophilic membranes have presented a suitable resistance. However, a prominent function has been presented by antibacterial expletives in boosting the resistance of the membrane to the joined organisms [8]. Javadi et al. showed a boost in hydrophilicity and membranes' water flow with the addition of hydrophilic ND nanoparticles. It has been indicated by the conclusion that a rise is seen in friction- and fouling-resistant membranes with the presence of ND nanoparticles [9]. Kumar et al. included a GO-TiO_2 nanocomposite as a hydrophilic additive to upgrade antifouling features of PSf ultrafiltration membranes. The inclusion of a GO-TiO_2 nanocomposite has proven to enhance the hydrophilicity of compound membranes. Besides, the rising levels of GO-TiO_2 have been linked to reduced irretrievable HA sediment [10]. Silver nanoparticles have been known for their exceptional chemical and mechanical traits, which have largely captured the attention of researchers due to the possible probes in their applications in nanomedicine, varying from antimicrobial [11] to drug delivery [12] to alleviation of injuries [13]. The highest bactericidal function and biocompatibility have also been observed in Ag nanoparticles, compared to all the other antibacterial nanomaterials [14, 15]. In fact, they have been utilized to reduce membrane biofouling because of their biocidal impacts [16-18]. Huang et al. collected silver nanoparticles in order to enhance the penetrance, antifouling, and antibacterial traits of ultrafiltration membranes. Significant antibacterial and antibiofouling performance was then observed from the membrane containing Ag nanoparticles, against *E. coli* and *B. subtilis* [19].

Two central challenges in the use of these nanoparticles in membrane applications have been the release and accumulation of Ag. GO is known as a highly oxidized graphene sheet, containing various oxygen-carrying functional groups (carboxyl, hydroxyl, and epoxy groups) which are located on the fundamental surface and on the brinks [20]. The most significant factor behind the intense hydrophilicity of GO is deemed to be these chemical functional groups. This characteristic, along with their wide surface, has made these nanosheets more likely to be utilized as a supplement for polymeric membranes for addressing the fouling issue [21-23]. Suitable nucleation spots for silver nanoparticles are obtained from GO functional groups. Ag nanoparticles, as a result, can firmly bind to the plate of GO. Silver nanoparticles have been collected on graphene oxide sheets (GO-Ag) in order to be utilized as a hydrophilic and antibacterial factor. GO-Ag compounds, therefore, are known as influential antibacterial substances with features similar to both GO and Ag nanoparticles. The general function of membranes could be improved with the help of GO-Ag in many ways, including their antibacterial characteristics and the hydrophilicity of their surface. Li et al. created PVDF membranes that presented marvelous penetrance and antibacterial quality, using GO-Ag nanoparticles as antibacterial substances [24].

Polysulfone (PSf) has been known as one of the most widely utilized polymer substances in membrane purification systems, compared to other developed membranes based on polymers. This is owing to its outstanding resistance to heat, chemical compatibility, and mechanical strength [25]. Several studies have referred to combining Ag nanoparticles with PSf membranes to avoid microbial propagation. The impact of silver nanoparticles on the antibacterial and antifouling properties of polysulfone nanocomposite membranes has been investigated by Ali et al. [26]. Xu et al. also developed PSf ultrafiltration membranes with the use of business Ag/Cu_2O hybrid nanowires with outstanding antimicrobial performance; the blended membranes held a remarkable antibacterial duration with very little release of Ag^+ [27]. PSf ultrafiltration membranes with Ag presented antimicrobial

traits against various types of bacteria, namely Escherichia coli and Pseudomonas mendocina [28]. An eye-catching waste of silver was seen, which consequently decreased antibacterial and antiviral performance.

This study focuses on the development of a PSf membrane combined with a GO-Ag nanocomposite. To sustain and control the release of Ag, a GO-Ag nanocomposite with significant mechanical strength, high antibacterial traits, and wide surface area was synthesized. GO-Ag nanohybrid was produced and then characterized using various analytical methods like UV, FESEM, EDX, and XRD. The produced GO-Ag nanocomposite was then fixed in the PSf matrix. Membranes were made with the use of the division methods of non-solvent-induced phase separation. Examinations were conducted on the anti-fouling qualities of membranes in the MBR system. To confirm the development in flow of infiltrate, antibacterial functions, and antifouling features in MBR systems, extensive analysis was conducted both operationally and structurally.

Although GO-Ag modified polymeric membranes have been previously reported for antibacterial and antifouling applications, most studies focus on bench-scale filtration tests using model foulants and do not address membrane performance under realistic MBR operating conditions. In contrast, the present work evaluates GO-Ag modified polysulfone membranes in a lab-scale membrane bioreactor treating activated sludge, with systematic analysis of critical flux, fouling behaviour, flux recovery, mechanical durability, and silver release. Furthermore, the role of graphene oxide as an anchoring matrix for suppressing Ag release is quantitatively demonstrated, and an optimal nanocomposite loading is identified. These features distinguish this study from earlier GO-Ag membrane reports and provide insight into the practical applicability of such membranes for long-term MBR operation.

2. EXPERIMENTAL

2.1. Materials

Slovay was chosen to provide business degree PSf (ρ=1250 kg.m^{-3}). N, N-dimethylacetamide (DMAc) was purchased from Merck to be utilized as solvent. Silver nitrate ($AgNO_3$) and Graphene Oxide nanosheets (99.50% purity, 1.5-5.5 µm sheet diameter, 0.43-1.23 nm width with 6-10 layers) were provided from US Research Nanomaterials Inc., and Polyethylene glycol (PEG, MW=20000) was supplied from Merck. Water flow was assessed using deionized (DI) water as an average and also as a non-solvent to enforce stage overturn. All the substances in these tests were diagnostic types and utilized exactly as they were obtained.

2.2. GO-Ag Nanocomposite Preparation

120 mL of DI water was used, in which 30 mg of GO was ultrasonically dissolved. GO was then ultrasonicated for one hour, and afterwards, 4 molar NaOH solution (10 mL) was added to the mixture drop by drop. This solution was then sonicated for more than 30 minutes so that a steady colloid of the suspension was developed as a result. The chemical reaction lasted for half an hour at a temperature of 70 °C, during which the color of the solution turned brown gradually. Being continuously stirred, 20 mg of $AgNO_3$ was then added to the mixture. At last, the solution was purified, cleaned 3 times with deionized water, and dried afterwards in a vacuum drier at 60 °C for 12 hours to gather the GO-Ag nanocomposite. The GO-Ag nanocomposite was prepared by chemically depositing silver (Ag) nanoparticles onto water-soluble GO sheets using NaOH (reducing agent). Ag-Ag nanostructures were formed when the Ag^+ ions were reduced during the reducing process, and the resulting Ag nucleated on the surface of GO sheets.

2.3. Membrane Preparation

The technique used in preparing the flat sheet membranes was the non-solvent induced phase separation (NIPS) method. To produce a homogeneous solution, varied degrees of GO-Ag (i.e., 0.10, 0.30, and 0.50 wt.%) were diffused in 75.00 wt.% DMAc to a sufficient degree. The mixture was then sonicated for 3 hours. The remaining 25 wt.% contained (15.00 wt.% PSf and nanoparticles) and (10.00 wt.% PEG). PSf and PEG polymers were added to the suspension and then blended for 12 hours at 60 °C, after ultrasonication for 3 h, so that a homogeneous solution was formed. To eliminate air bubbles, the molding solution was aired for 12 hours. A mechanized molding machine (Coa Test, Taiwan) was then used to cast the solution onto a glass plate to acquire a flat sheet polymeric membrane. The produced membrane was then instantly immersed in the coagulation bath at 30 °C to complete the phase inversion process. The synthesized membranes were then retained in deionized (DI) water to make sure that the remaining solvent was totally removed. Table 1 illustrates the combination of various polymeric solutions.

2.4. GO-Ag Nanocomposite Characterization

Different methods are applied to classify GO-Ag nanosheets, including ultraviolet–visible (UV–vis) absorption spectra, X-ray diffraction, field emission scanning microscope, and diffusive X-ray analysis (EDX) detector. Ag nanoparticles were evidently declared present, using UV-Vis spectroscopy, as a plasmon absorption band was detected. A Shimadzu UV-1650PC spectrometer was used to report the UV-visible spectra in the range between 200 and 800 nm. X-ray diffraction (XRD, D500 Siemens) in the scanning range of 2θ between 5° and 70° at an accelerating voltage of 45 kV. Morphologies of GO and GO-Ag nanoparticles were pictured using a Field Emission Scanning Electron Microscope (FESEM; MIRA3 FEG-SEM, Tescan). The distribution of the Ag elements in the GO-Ag

J Water Environ Nanotechnol, 2026, 11(3): 311-325
10.22090/jwent.2025.2076875.2001

Table 1. Compositions of the prepared membranes.

Membrane	PSf (wt.%)	GO-Ag (wt.%)	PEG (wt.%)	DMAc (wt.%)
M-0.00	15.00	0.00	10.00	75.00
M-0.10	14.985	0.015	10.00	75.00
M-0.30	14.955	0.045	10.00	75.00
M-0.50	14.925	0.075	10.00	75.00

Table 2. The operation conditions for the MBR test system.

Parameters	Values
MLSS, (mg/L)	6500-7500
Sludge retention time, SRT (day)	30
Hydraulic retention time, HRT (h)	37
Chemical oxygen demand (COD), (mg/L)	3000
Aeration, (L/min)	1
Temperature, (°C)	25

nanocomposite was further confirmed by EDX mapping analysis.

2.5. Membrane Characterization

The morphology of the produced membranes was visualized using a Field Emission Scanning Microscope (FESEM; MIRA3 FEG-SEM, Tescan). Examples of membranes were frozen in liquid nitrogen and then covered with gold by sputtering before being observed. Measurements of the hydrophilicity of membranes were taken using an interaction angle goniometer (PGX, Thwing-Albert Instrument Co., USA) and were examined three times; the average of 3 evaluations was presented as the result. Calculation of the mechanical power of membranes was done using a stretchable examination machine (Santam STM-5, Iran), and strained at a steady speed of 10 mm/min; the average figures for the samples (50 mm length and 10 mm width) were reported. For the friction resistance trial to be carried out, damp membranes were soaked in 50.00 wt.% silicon carbide suspension and then stirred continuously at 200 rpm for 7 days. All the samples were carefully weighed before and after the test to quantify the possible decline in weight because of erosion. The model of the membrane was, in the end, cleaned under ultrasonication for 20 minutes to remove the suspension from the membrane for examination.

2.6. Antibacterial Test

Investigations were also conducted on the antibacterial function of the synthesized membranes by the technique referred to elsewhere with the use of *E. coli* bacteria [19, 29]. The applied *E. coli* bacteria suspension was developed at 37 °C and constantly shaken at 150 rpm for 12 hours in Luria-Bertani (LB). For assessing the antibacterial properties, membranes were placed on Luria–Bertani (LB) agar plates of E. coli developed at 37 °C for 24 hours to fix the concentration of E. coli at 106 CFU/mL. Halo sites were created around models after 24 hours, which signal reversed anti-bacterial zones linked to the presence of GO-Ag nanoparticles.

2.7. Release Test

Release of silver nanoparticles in nature is a possible major issue. A method highly recommended by recent studies to better regulate the release degrees has been the combination of Ag nanoparticles with different organic or inorganic matrices. To estimate the release of silver from the membrane matrix with time, samples were soaked in water at room temperature. To create a simulation of the work environment, water with a mixer was applied to form a stream. At the end of the first, second, and third week, modelling was done. Ag released from the GO-Ag nanocomposite membrane was evaluated by inductively Coupled Plasma (ICP-OES (Thermo Scientific DUO 6500) [30].

2.8. Pure Water Flux and MBR Setup

Table 2 illustrates the operational conditions of the MBR, which was a lab-scale membrane bioreactor (MBR) setup used in this work. For calculating the water flow of synthesized membranes, the membrane sample was soaked in a water tank that was linked to a vacuum pump so that a transmembrane pressure of 0.7 bar could be supplied. PWF was calculated by:

$$J_0 = \frac{V}{At} \quad (1)$$

where J_0 is the penetration flow of membrane for unadulterated water flux (L/m²h), V is compact volume of

water (L), A is membrane's effective surface area (m^2), and t is time (h). The analytical flow was assessed by the TMP-step technique, in which TMP rises throughout the time (45 min at each TMP step); the first uneven spot was observed when J declined with time, which resulted in a nonlinearity in flux-TMP association [31]. The membrane sample was submerged in the MBR system after computing the PWF (J_0). Measurements of the flow of activated sludge purification were based on penetration weight at subcritical and fixed TMP conditions for 360 minutes. The sample of the membrane was then removed from the MBR and soaked in the water tank to calculate the PWF of fouled membranes (J_1). The cover layer on the surface of the membrane was subsequently washed with DI water. PWF of the membrane was then calculated again (J_2). The following equations were used to work out fouling qualities [32]:

$$TFR = \frac{J_0 - J_1}{J_0} \quad (2)$$

$$RFR = \frac{J_2 - J_1}{J_0} \quad (3)$$

$$IFR = \frac{J_0 - J_2}{J_0} \quad (4)$$

$$FRR = \frac{J_2}{J_0} \quad (5)$$

Where total fouling ratio (TFR), reversible fouling ratio (RFR), irreversible fouling ratio (IFR), and flux recovery ratio (FRR) [32].

2.9. COD Removal

CODs of effluent (COD_E) and influent (COD_I) were evaluated to quantify COD removal, based upon the absorbance technique and with the help of the following equation:

$$COD\ removal\,(\%) = \left(1 - \frac{COD_E}{COD_I}\right) \times 100 \quad (6)$$

3. RESULTS AND DISCUSSION

3.1. Characterization of GO-Ag Nanocomposite

The UV-Vis spectrum of GO and GO-Ag nanocomposite is illustrated in Fig. 1. A distinguished peak is shown at 300 nm in the UV-Vis spectrum of graphene oxide, which is linked to the n-π* electronic transition of the double bond of carbon-oxygen [33]. A peak was observed at 410 nm in the GO-Ag model, which was linked to Surface Plasmon Resonance (SPR) for silver. This illustrates the creation of silver nanoparticles on the graphene oxide nanosheets [34, 35].

The combination of Ag nanoparticles with the nanocomposite was also confirmed by the XRD analysis (Fig. 2). A noticeable peak, which is a typical one of GO, appears at 2θ = 10.8 ° [22]. The peaks detected at 2θ = 38.1 °, 44.3°, 69.6°, and 77.4° are respectively assigned to the (111), (200), (220), and (311) crystalline planes from crystalline silver nanoparticles [36, 37]. The peak concentration of the GO index declined in the GO-Ag model and changed a little from 2θ = 10.8° to 2θ = 9.6°. This verifies the rise in inter-spacing of the GO-Ag nanocomposite, which occurred because of the location of Ag between GO sheets. Attachment of Ag nanoparticles to the GO sheets, as a result, stops GO layers from being stacked [38]. The factor behind this circumstance is the presence of Ag nanoparticles between GO layers, which has created an ideal space between layers that could potentially enhance the hydrophilicity features of nanoparticles.

FESEM analysis of the GO and GO-Ag nanocomposites was conducted to detect the structure of nanoparticles. Fig. 3 illustrates spherical silver nanoparticles that are spherical shaped and were successfully fixed on the GO surface, which has a thin and planar structure. The identity of particles was verified by

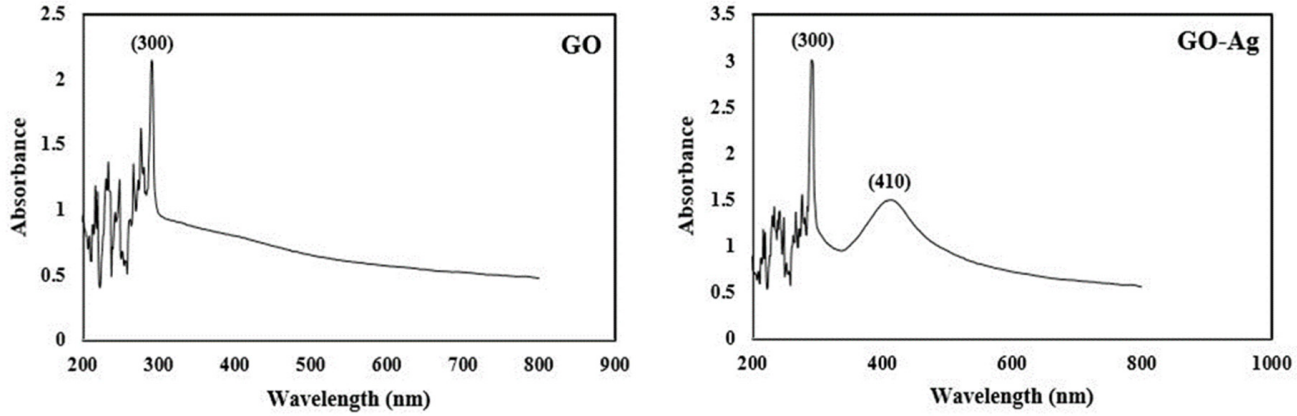

Fig. 1. UV–vis spectra of GO and GO-Ag nanoparticles.

J Water Environ Nanotechnol, 2026, 11(3): 311-325
10.22090/jwent.2025.2076875.2001

Dot. Mapping analysis. Red zones in the figure illustrate the dispersion of Ag, and this indicates that silver nanoparticles were distributed homogeneously through the GO-Ag nanocomposite. No changes were also seen in the structure of GO with hydrophilic functional groups, with silver ornamented on the GO. The production of the GO-Ag nanocomposite was evidently confirmed by these conclusions.

3.2. Membrane Morphology

The impact of attaching nanoparticles to the structure of membranes (Fig. 4) was investigated with the help of surface and cross-section pictures of the neat and nanocomposite membranes detected by FESEM. The number of surface models of the neat PSf membrane is seen to be much lower than that of the nanocomposite membrane. Larger holes could be detected as the concentration of GO-Ag nanocomposite was raised from 0.10 to 0.50 wt.%. GO-Ag nanocomposite was seen to act like a hydrophilic stabilizer that influenced the speed of exchange between solvent and non-solvent during phase division. This eventually triggered the creation of bigger hole channels [39, 40]. Sponge-like pores could be detected in cross-section FESEM images (right column of Fig. 4) as the concentration of GO-Ag nanocomposites was raised. As illustrated in the right column of Fig. 4, all membranes had a typically asymmetric permeable structure with a thick skin and a sponge resembling top-layer that was accompanied by a finger-like leaky sub-layer. The regular membrane had a thick hole channel on the top layer and a loose pore channel on the lowest layer. As the amount of GO-Ag in membranes rose from 0.10wt.% to 0.50wt%, the sponge-like section on the lowest layer increased in comparison with the neat PSf membrane, while the quantity of finger-like holes had a slow decline. This condition could be explained by the hydration of functional groups on the polar side of GO and Ag that consequently reduces the exchange rate of water molecules and solvent molecules; the first water molecules reaching the surface would be engaged in hydrating and bonding with the functional groups of GO and Ag on the surface. This finally captures the space around the membrane and reduces the exchange rates referred to above. As a result of this condition, smaller holes and sponge-voids will be formed [41].

3.3. Antibacterial Properties

According to Fig. 5, examinations that aimed to evaluate the antibacterial traits indicated that neat PSf membranes (M-0.00) did not show any antibacterial performance. This was confirmed by the growth of bacteria near the surface of the membrane. The nanocomposite membranes, on the contrary, presented a dark loop, which indicated the reverse areas against E. coli for the GO-Ag nanocomposite membrane. A legitimate explanation for this antibacterial impact is the contact between GO and Ag on the surface of the membrane, which prohibited

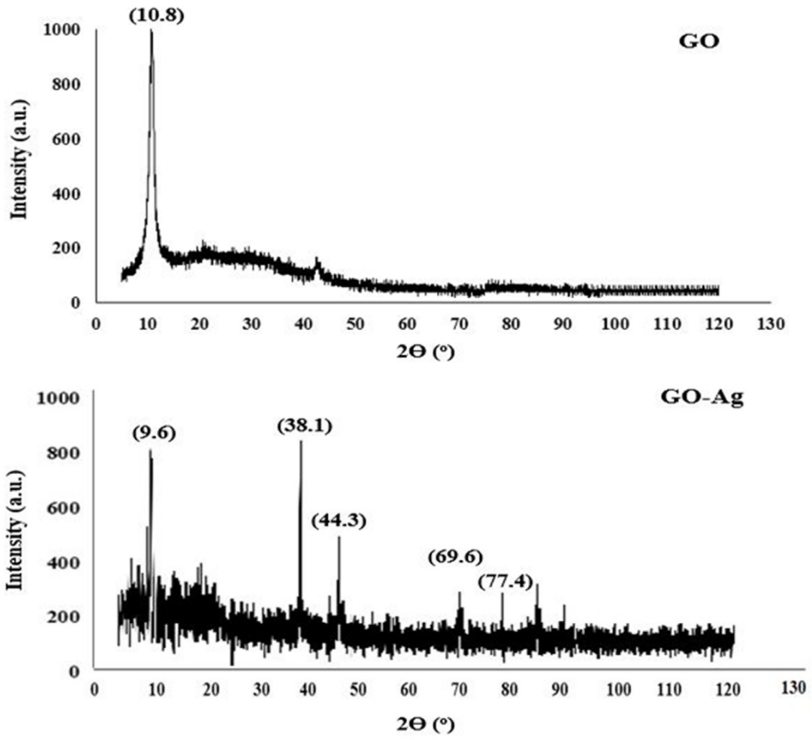

Fig. 2. XRD patterns of GO and GO-Ag nanoparticles.

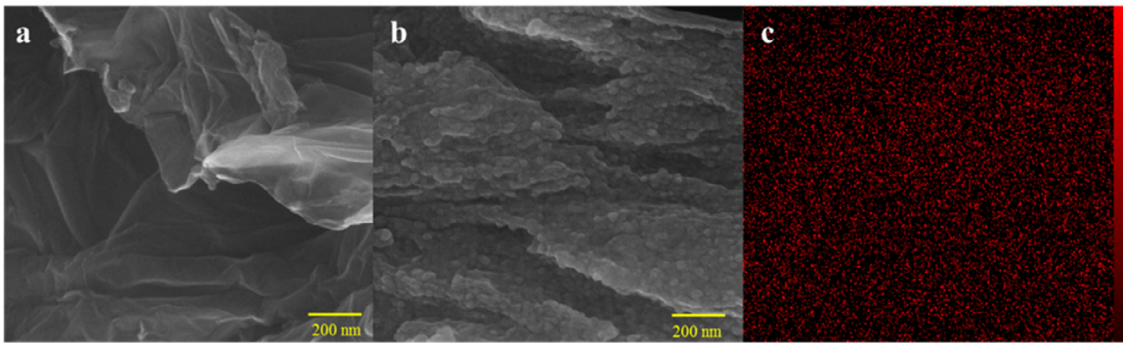

Fig. 3. FESEM images of a) GO and b) GO-Ag, and EDX-Mapping of c) GO-Ag nanoparticles.

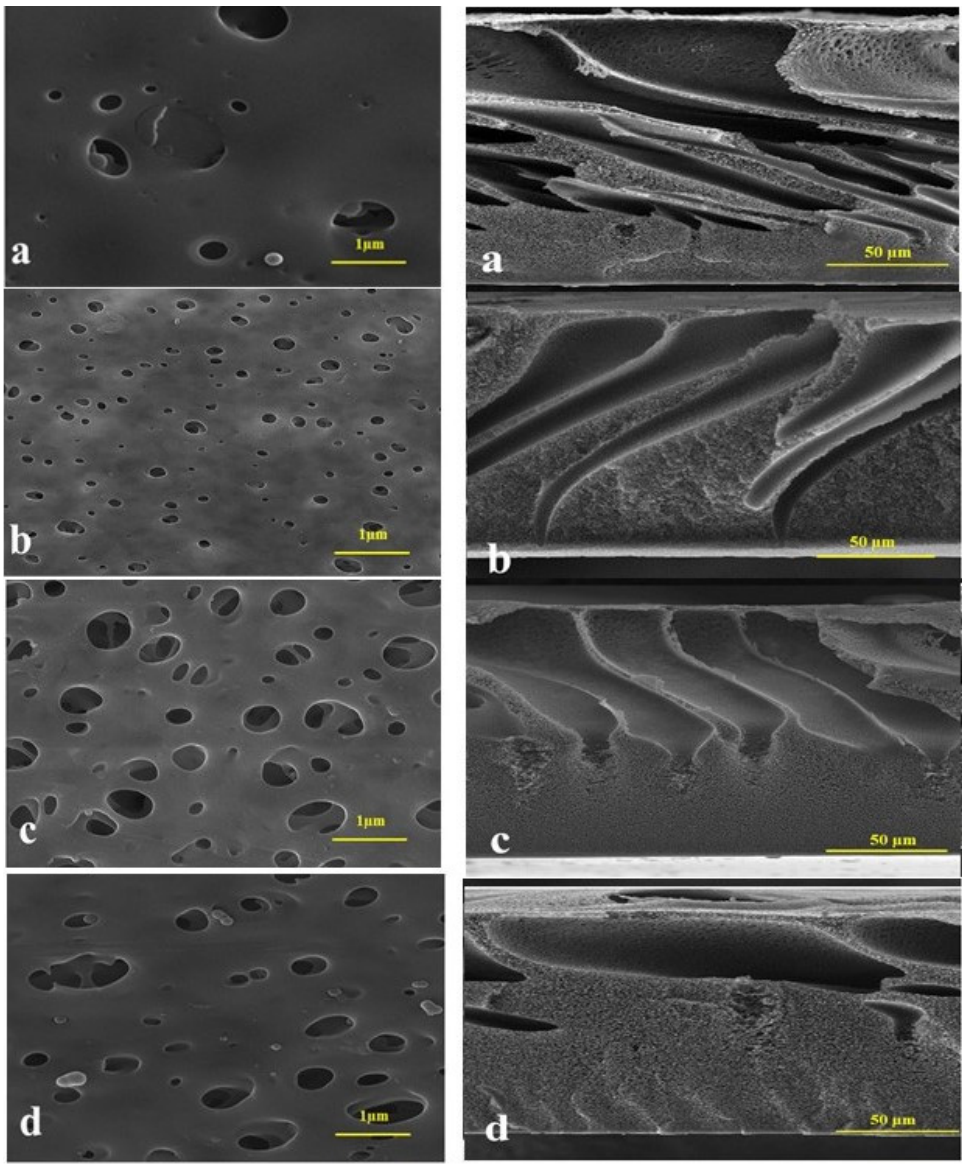

Fig. 4. Surface (left) and cross-sectional (right) FESEM images of prepared membranes: a) M-0.00, b) M-0.10, c) M-0.30 and M-0.50.

J Water Environ Nanotechnol, 2026, 11(3): 311-325
10.22090/jwent.2025.2076875.2001

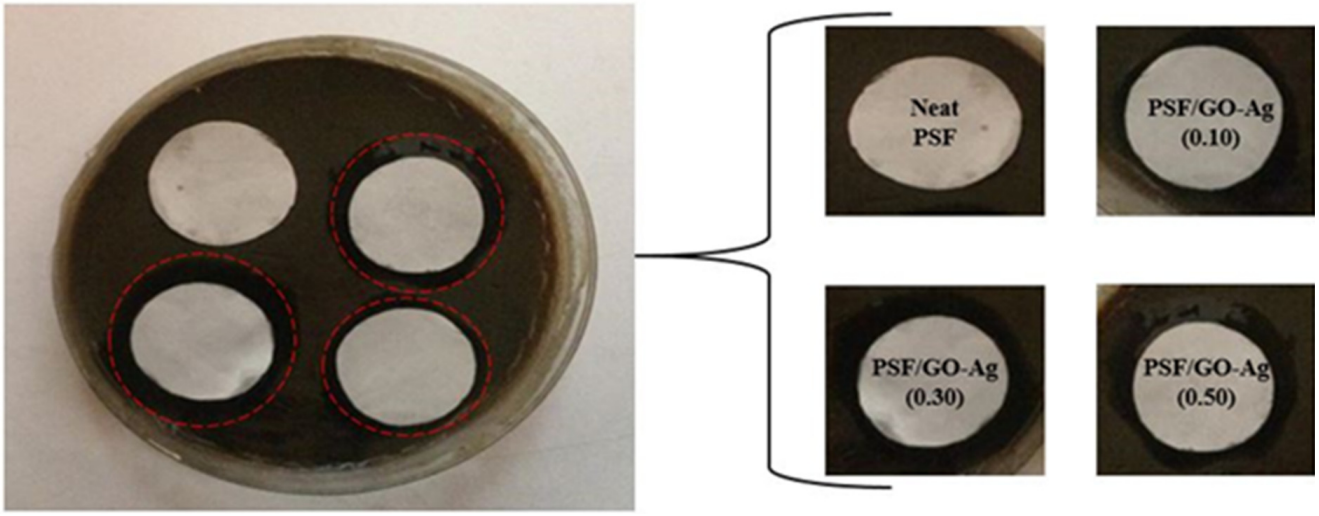

Fig. 5. Antibacterial activity of different samples.

the release of Ag in the zone near the nanocomposite-modified membrane.

Since silver nanoparticles are less detached from the GO surface, the underlying mechanism for the antibacterial quality of silver in the membrane matrix should not be linked to the release of silver from the GO-Ag nanocomposites. The synthesized GO-Ag was declared good for a secure antibacterial function, since the release of Ag leads to immobility of Ag nanoparticles in a significant structure of GO. The factors behind silver's antibacterial function and its mechanism in these sorts of usages remain unexplained. The antibacterial function of Ag nanoparticles has been linked to the contact between Ag nanoparticles and the thiol groups in enzymes and proteins. However, other qualities like hydrogen bonding could be influential as well [42, 43]. But several other papers have outlined that the mechanism behind the antibacterial function of Ag nanoparticles was because Ag nanoparticles dissolved to Ag^+ cations, which were capable of crashing the proton motive force and causing the death of the cell [44-46]. In our study, GO nanosheets were used to decrease the release of Ag nanoparticles. The antibacterial performance, as a result, has less potential to be linked to the interaction of bacteria with Ag nanoparticles. The antibacterial mechanism of the produced nanocomposite is solely based upon the antibacterial feature of Ag and is said to be worth deeper probes.

3.4. Mechanical Properties and Abrasion Resistance

The impacts that abrasive substances have on the polymeric membranes are a major issue, and the membranes that are resistant to abrasion are anticipated to reduce the maintenance expenses of membranes in the MBR system. Therefore, the mechanical power of membranes was assessed after an abrasion test. It could be detected that the insertion of GO-Ag nanocomposite into the PSf membrane enhanced resistance to membrane abrasion. However, a slight decrease was seen in the weight of membranes with rising degrees of GO-Ag. This can be attributed to the outstanding firmness and resistance of carbonaceous substances like GO [47]. In an experiment, abrasion resistance of cellulose acetate (CA) was enhanced using nano diamond. The results illustrated an improvement in CA membrane resistance against abrasive substances due to the outstanding stiffness and resistance of nanodiamond [48]. Abrasion resistance of membranes could also be evaluated using mechanical qualities. In this study, both elastic power and extension of synthesized membranes were quantified before and after the abrasion test, as listed in Table 3. The elastic power of a membrane rose as GO-Ag was added; however, the extension remained the same. This means that with GO-Ag, the mechanical strength of the PSf membrane was enhanced, which could be attributed to the strong structure of graphene oxide. Additionally, with 0.30 wt.% GO-Ag, the elastic strength was boosted from 5.60 MPa in the neat membrane to 6.56 MPa in the nanocomposite membrane, while the extension ratio remained steady.

Tensile intensities of the membranes fell after the abrasion test, but this reduction was more significant for the neat PSf membrane. Furthermore, mechanical features of nanocomposite membranes increased with a rise in the level of GO-Ag after the abrasion test. This implies that adding GO-Ag nanocomposite improved the abrasion resistance. Besides, nanoparticles supplied the physical reinforcement for the

Table 3. Mechanical properties of the prepared membranes before and after abrasion test.

Before abrasion test			After abrasion test	
Membrane	Tensile, MPa	Elongation, (%)	Tensile, MPa	Elongation, (%)
M-0.00	5.60	30.24	4.50	28.00
M-0.10	6.12	28.02	5.53	27.52
M-0.30	6.56	29.50	6.00	27.00
M-0.50	6.22	32.10	5.92	28.62

Table 4. Pure water flux, contact angle and weight loss after abrasion test.

Sample	PWF (L/m^{2}h)	Contact angle (°)	Weight loss (g/m^2)
M-0.00	80	82.5	31
M-0.10	95	65.3	27
M-0.30	190	51.6	19
M-0.50	178	53.4	17

structure of the membrane. GO has been studied to determine whether it could be used as a nanofiller that could upgrade its mechanical traits for nanocomposite membranes [49].

3.5. Pure Water Flux and Hydrophilicity

Table 4 provides information on pure water flow, angle of water interaction, and weight loss of the synthesized membranes after abrasion. The incorporation of GO-Ag nanocomposite caused a decline in water contact angle, which could be linked to the basic hydrophilic properties of oxygen functional groups in this nanocomposite. The nanocomposite membranes showed good hydrophilic characteristics compared to the neat membranes. It should be noted that among all modified membranes, the lowest value for contact angle (51.6°) was obtained for M-0.30. Additionally, the uniform distribution of nanocomposite leads to a noticeably enhanced percentage of pure water flux of PSf/GO-Ag membranes, over that of neat PSf membranes. Pure water flux rose from 74 L/m^{2}h for the M-0.00 membrane to approximately 190 L/m^{2}h MH for M-0.30. The consequent rise in the membrane's PWF due to GO-Ag nanocomposite addition could be attributed to the nucleation influence of nanoparticles. Besides, as illustrated in FESEM images, an increase in GO-Ag could lead to an increase in the size of surface holes as well as a decrease in the number of surface pores, but eventually provides more space needed for water penetration. The increase in hydrophilicity could be essential in boosting the penetrance and anti-fouling qualities of the membrane.

3.6. Critical Flux Measurement and MBR

Fig. 6 illustrates the results gathered from the detection of the major flow of produced membranes, using the TMP-step technique. The capture of two straight lines with various slopes in the flux-TMP chart is regarded as the critical flux/TMP point. These results indicate the impact of GO-Ag nanocomposite on the major flow of PSf membranes. In the presence of GO nanosheets, membrane hydrophilicity is improved, and interaction between foulants and the surface of the membrane is reduced. Besides, Ag with antibacterial qualities prohibits the accumulation of bacteria on the surface of the membrane. Eventually, the combination of hydrophilic GO-Ag nanocomposite reduces the contact between fouling elements and the surface of the membrane, which leads to an improvement in the major flow, compared to the neat membrane [28].

Fig. 7 provides information on the flow decrease performance that synthesized membranes show during the MBR process. All purification tests were conducted at a subcritical pressure of 0.1 bar and processed until the flow reached a fixed amount. Initially, evaluations were conducted on the flow of unadulterated water for 90 minutes, and then purification of the MBR was carried out for another 360 min. The surface of the membrane was then rinsed physically, and clean water flow was assessed again in order to evaluate fouling parameters. The initial flow of the GO-Ag nanocomposite membrane was observed to be more than that of the neat PSf membrane. From M-0.00 membrane, however, flow began from 70 L/m^{2}h and then fell to 22 L/m^{2}h after 360 min. In the case of the M-0.30 membrane, the early and final obtained figures for flow were correspondingly 178 and 136 L/m^{2}h, which indicates that the antifouling function of PSf/GO-Ag membranes rose considerably because the GO-Ag nanocomposite was present. This could be attributed to the hydrophilicity and antibacterial

J Water Environ Nanotechnol, 2026, 11(3): 311-325
10.22090/jwent.2025.2076875.2001

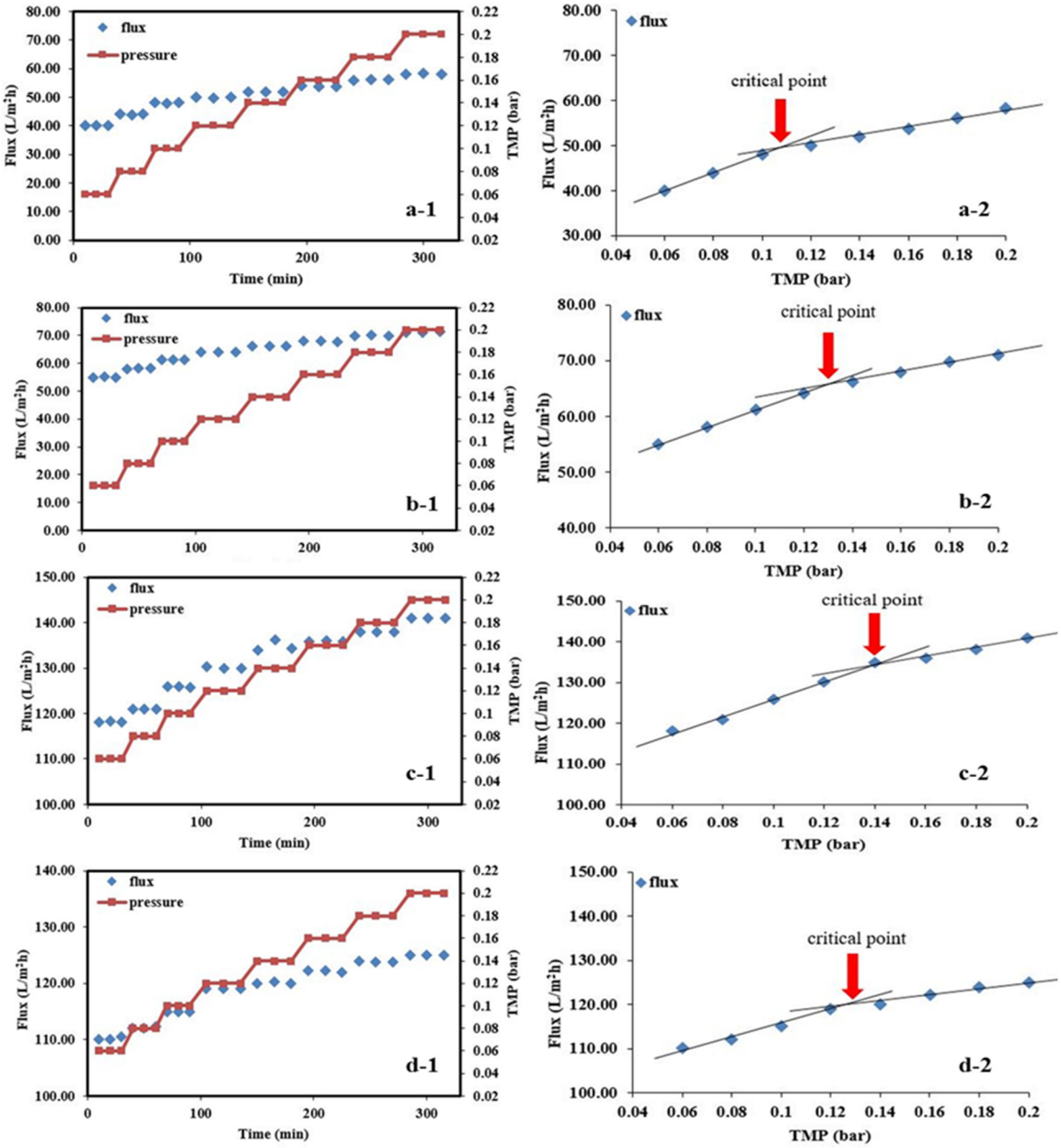

Fig. 6. Determination of the critical flux by the TMP-step method for M-0.00 (a-1 and a-2), M-0.10 (b-1 and b-2), M-0.30 (c-1 and c-2) and M-0.50 (d-1 and d-2).

features of the GO-Ag nanocomposite that cause a decline in the adsorption of hydrophobic foulants like proteins on the surface of the membrane [50, 51].

3.7. Antifouling Performance and Rejection

Fig. 8 provides information on fouling parameters including TFR, RFR, IFR, and FR that could label the antifouling attributes of prepared membranes. As both membranes were examined under the same circumstances, the diverse fouling qualities could be attributed to the influence of the GO-Ag nanocomposite on the membrane antifouling feature. Compared to all membranes, the M-0.30 membrane presented the most reversible sediment that could be easily eliminated by rinsing with pure water, since the antifouling performance of GO-Ag intensely prohibits the foulants from attaching to the surface of the membrane [28]. Fig. 8 illustrates that the GO-Ag nanocomposite reduced TFR from 87.75% for the neat PSf

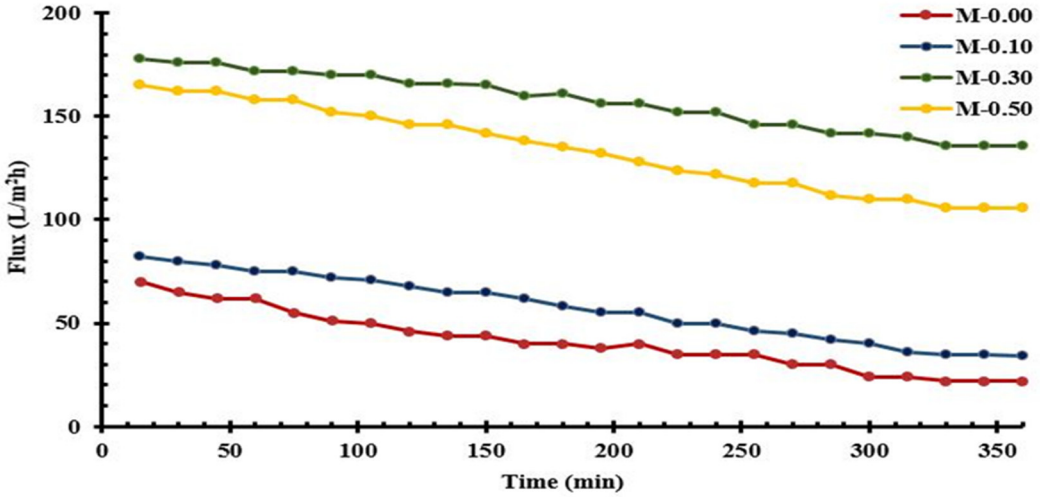

Fig. 7. Flux-time behavior of prepared membranes in MBR.

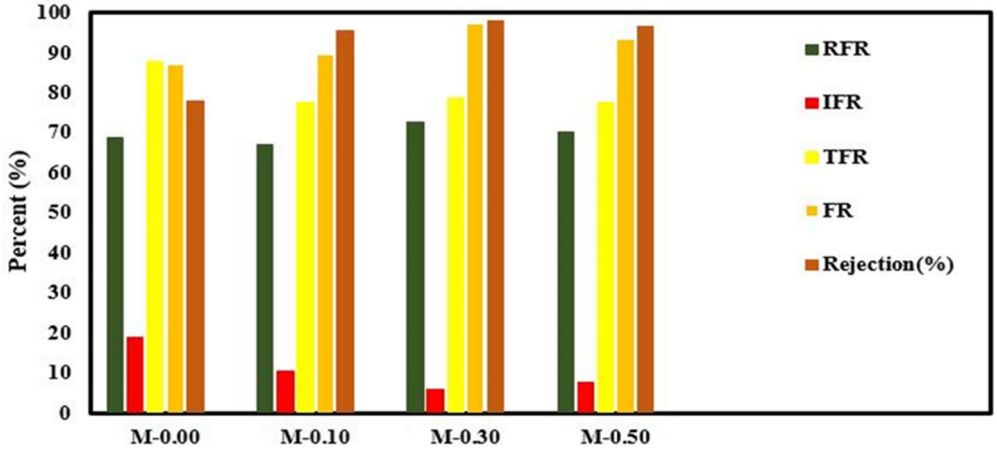

Fig. 8. Fouling parameters of prepared membranes during activated sludge filtration.

membrane to 78.58% for the 0.30 wt.% GO-Ag established membrane. Additionally, IFR of produced membranes fell from 18.97% for M-0.00 to 5.98% for M-0.30 membrane. It could be declared, additionally, that combining GO-Ag nanocomposite with PSf membranes boosted the resistance to fouling. Adding hydrophilic nanoparticles to the membrane matrix, as a result, enhanced the hydrophilicity of the membrane and created a very thin layer of water on the surface of the membrane that decreased the hydrophobic sorption of sludge particles. Therefore, an improvement in hydrophilicity is expected to reduce membrane fouling and increase the recovery of flow. Also, Fig. 8 illustrates COD removal (rejection). COD removal of all nanocomposite membranes was higher than 95.00%; however, removal in the conventional activated sludge (CAS) bioreactor, which is only carried out by biological activities, was only 82.40% efficient. In the MBR system, this process continues with membrane purification. COD elimination in nanocomposite membranes was higher than that of the neat PSf membrane. This could be linked to hydrophilicity and antibacterial features of nanocomposite membranes.

In MBR systems, COD removal is primarily achieved through biological degradation, with the membrane mainly used for solid–liquid separation and ensuring complete biomass retention. Although the membrane does not directly reject dissolved COD, it contributes to stabilizing biological performance by sustaining high MLSS concentrations and preventing biomass washout. The modest improvement in COD removal observed with GO–Ag modified membranes can

J Water Environ Nanotechnol, 2026, 11(3): 311-325
10.22090/jwent.2025.2076875.2001

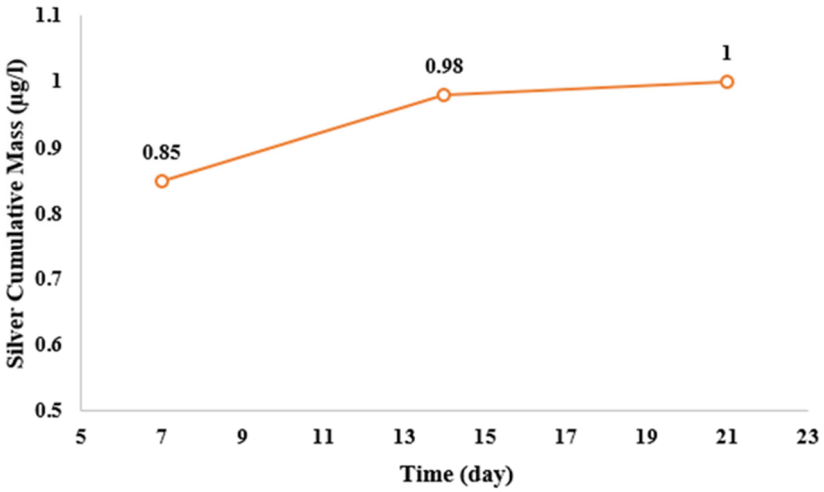

Fig. 9. Ag release concentration per day.

be attributed to their superior fouling resistance and sustained flux, which together foster more stable filtration conditions. This behaviour differs from CAS, where COD removal relies solely on biological activity and is generally lower due to the absence of membrane-assisted biomass retention.

3.8. Release analysis

Fig. 9 provides information on the daily concentration of Ag release from the excellent membrane, M-0.30. Data analysis was done physically by organizing the increasing mass with time. Silver was quickly released at the beginning of the test, and initially, a concentration of 0.85 µg/l was released on the first day.

Considering the general trend in total release of Ag nanoparticles over time, it was declared that releases in the second and third week were significantly lower than those of nanoparticles compared to the early days. It could be indicated from Fig. 9 that the condensation of release remained constant for seven days (about 1µg/l), which is a sign of balance in release from the membrane in that environment. The final concentration of Ag could reach 1 µg/l, while more than 92.00% of the total silver would still be in the nanocomposite structure. As a matter of fact, this happens because silver nanoparticles would be formed on the surface of the nanocomposite.

4. CONCLUSION

This study demonstrates that functionalizing Ag nanoparticles with graphene oxide nanosheets and incorporating the resulting GO–Ag nanocomposite into PSf membranes is an effective strategy to impart hydrophilic and antibacterial properties while improving antifouling performance. The PSf/GO–Ag membranes exhibited enhanced flux, hydrophilicity, antibacterial activity, abrasion resistance, and foulant rejection, with the optimal formulation (M-0.30) achieving ~99% rejection and retaining ~92% of Ag after three weeks. FESEM and EDX analyses confirmed the uniform dispersion of Ag on GO, while UV and XRD validated structural variations induced by GO incorporation. Beyond these results, the findings provide important design implications: excessive nanoparticle loading does not proportionally improve performance and may compromise membrane morphology, highlighting the need for controlled nanofiller incorporation rather than maximum addition. From a scalability perspective, the enhanced abrasion resistance, sustained flux, and suppressed silver release suggest that GO–Ag modified membranes could extend operational lifetimes, reduce cleaning frequency, and ensure safer long-term use in full-scale MBR systems. Overall, the study establishes a framework for designing durable, high-performance membranes that balance functionality with material economy. GO–Ag modified PSf membranes thus represent a practically viable option for advanced wastewater treatment, offering both scientific innovation and industrial relevance.

Conflict of Interest
The authors declare no conflict of interest.

Funding
This study was not supported by any funding.

Author's Contributions
Study Conception or Design: Samaneh Kazemi, Yoones Jafarzadeh, Reza Yegani
Data Acquisition: Samaneh Kazemi
Data Analysis or Interpretation: Soroush Khakpour
Manuscript Drafting: Soroush Khakpour
Critical Manuscript Revision: Yoones Jafarzadeh, Reza Yegani
All authors have approved the final manuscript and are responsible for all aspects of the work.

AI Statement
The authors confirm that no AI tools or services were used during the preparation of this work.

REFERENCES

1. Onagh S, Hazrati H, Jafarzadeh Y (2024) Application of modified PVC membranes with GO-ZnO nanoparticles in MBR: Sludge characteristics, fouling control and removal performance. J Tw Ins Chem Eng 162:105586. https://doi.org/10.1016/j.jtice.2024.105586
2. Rashidi R, Khakpour S, Masoumi S, Jafarzadeh Y (2022) Effects of GO-PEG on the performance and structure of PVC ultrafiltration membranes. Chem Eng Res Des 177:815-825. https://doi.org/10.1016/j.cherd.2021.11.021
3. Mutamim NSA, Noor ZZ, Hassan MAA, Yuniarto A, Olsson G (2013) Membrane bioreactor: Applications and limitations in treating high strength industrial wastewater. Chem Eng J 225:109-119. https://doi.org/10.1016/j.cej.2013.02.131
4. Zhao L, Wu L, Lu X, Ng D, Truong YB, Xie Z (2018) Activated carbon enhanced hydrophobic/hydrophilic dual-layer nanofiber composite membranes for high-performance direct contact membrane distillation. Desalination 446:59-69. https://doi.org/10.1016/j.desal.2018.09.002
5. Wang H, Wang W, Wang L, Zhao B, Zhang Z, Xia X, Yang H, Xue Y, Chang N (2018) Enhancement of hydrophilicity and the resistance for irreversible fouling of polysulfone (PSF) membrane immobilized with graphene oxide (GO) through chloromethylated and quaternized reaction. Chem Eng J 334:2068-2078. https://doi.org/10.1016/j.cej.2017.11.135
6. Zhang G, Zhou M, Xu Z, Jiang C, Shen C, Meng Q (2019) Guanidyl-functionalized graphene/polysulfone mixed matrix ultrafiltration membrane with superior permselective, antifouling and antibacterial properties for water treatment. J Colloid Interf Sci 540:295-305. https://doi.org/10.1016/j.jcis.2019.01.050
7. Li R, Wu Y, Shen L, Chen J, Lin H (2018) A novel strategy to develop antifouling and antibacterial conductive Cu/polydopamine/polyvinylidene fluoride membranes for water treatment. J Colloid Interf Sci 531:493-501. https://doi.org/10.1016/j.jcis.2018.07.090
8. Meng F, Zhang S, Oh Y, Zhou Z, Shin HS, Chae SR (2017) Fouling in membrane bioreactors: An updated review. Water Res 114:151-180. https://doi.org/10.1016/j.watres.2017.02.006
9. Javadi M, Jafarzadeh Y, Yegani R, Kazemi S (2018) PVDF membranes embedded with PVP functionalized nanodiamond for pharmaceutical wastewater treatment. Chem Eng Res Des 140:241-250. https://doi.org/10.1016/j.cherd.2018.10.029
10. Kumar M, Gholamvand Z, Morrissey A, Nolan K, Ulbricht M, Lawler J (2016) Preparation and characterization of low fouling novel hybrid ultrafiltration membranes based on the blends of GO–TiO2 nanocomposite and polysulfone for humic acid removal. J Membr Sci 506:38-49. https://doi.org/10.1016/j.memsci.2016.02.005
11. Singh PK, Bhardwaj K, Dubey P, Prabhune A (2015) UV-assisted size sampling and antibacterial screening of Lantana camara leaf extract synthesized silver nanoparticles. RSC Advances 5:24513-24520. https://doi.org/10.1039/C4RA17233G
12. Sahoo SK, Misra R, Parveen S (2017) Nanoparticles: a boon to drug delivery, therapeutics, diagnostics and imaging. Nanomedicine: Nanotechnology, Biology and Medicine 8:73-124. https://doi.org/10.1016/j.nano.2011.05.016
13. Rigo C, Ferroni L, Tocco L, Roman M, Munivranab L, Gardin C, Cairns W, Vindigni V, Azzena B, Barbante C (2013) Active Silver Nanoparticles for Wound Healing. Int J Mole Sci 14:4817-4840. https://doi.org/10.3390/ijms14034817
14. Liang H, Wang H, Sun X, Xu W, Meng N, Zhou N (2023) Development of ZnO/Ag nanoparticles supported polydopamine-modified montmorillonite nanocomposites with synergistic antibacterial performance. Appl Clay Sci 244:107112. https://doi.org/10.1016/j.clay.2023.107112
15. Knetsch MLW, Koole LH (2011) New Strategies in the Development of Antimicrobial Coatings: The Example of Increasing Usage of Silver and Silver Nanoparticles. Polymers 3:340-366. https://doi.org/10.3390/polym3010340
16. Behboudi, A, Jafarzadeh, Y, Yegani, Y (2018) Enhancement of antifouling and antibacterial properties of PVC hollow fiber ultrafiltration membranes using pristine and modified silver nanoparticles, J. Environ. Chem. Eng. 6 (2): 1764-1773. https://doi.org/10.1016/j.jece.2018.02.031
17. Ananth A, Arthanareeswaran G, Ismail AF, Mok YS, Matsuura T (2014) Effect of bio-mediated route synthesized silver nanoparticles for modification of polyethersulfone membranes. Colloids Surf. A: Physicochem Eng Asp 451:151-160. https://doi.org/10.1016/j.colsurfa.2014.03.024
18. Behboudi, A, Jafarzadeh, Y, Yegani, Y (2018) Incorporation of silica grafted silver nanoparticles into polyvinyl chloride/polycarbonate hollow fiber membranes for pharmaceutical wastewater treatment, Chem. Eng. Res. Des. 135: 153-165. https://doi.org/10.1016/j.cherd.2018.03.019
19. Huang L, Zhao S, Wang Z, Wu J, Wang J, Wang S (2016) In situ immobilization of silver nanoparticles for improving permeability, antifouling and anti-bacterial properties of ultrafiltration membrane. J Membr Sci 499:269-281. https://doi.org/10.1016/j.memsci.2015.10.055
20. Khakpour S, Jafarzadeh Y, Yegani R (2019) Incorporation of graphene oxide/nanodiamond nanocomposite into PVC ultrafiltration membranes. Chem Eng Res Des 152:60-70. https://doi.org/10.1016/j.cherd.2019.09.029
21. Goyat R, Singh J, Umar A, Saharan Y, Ibrahim AA, Akbar S, Baskoutas S (2024) Synthesis and characterization of nanocomposite based polymeric membrane (PES/PVP/GO-TiO2) and performance evaluation for the removal of various antibiotics (amoxicillin, azithromycin & ciprofloxacin) from aqueous solution. Chemosphere 353:141542. https://doi.org/10.1016/j.chemosphere.2024.141542
22. Zhao Y, Lu J, Liu X, Wang Y, Lin J, Peng N, Li J, Zhao F (2016) Performance enhancement of polyvinyl chloride ultrafiltration membrane modified with graphene oxide. J Colloid Interf Sci 480:1-8. https://doi.org/10.1016/j.jcis.2016.06.075
23. Ghasemzadeh F, Kazerouni HN, Adelinia H, Jafarzadeh Y, Hazrati H (2023) Modified Graphene Oxide/Polyvinyl Chloride Membranes for Wastewater Treatment. Chem Eng Technol 46:373-382. https://doi.org/10.1002/ceat.202200333
24. Li J, Liu X, Lu J, Wang Y, Li G, Zhao F (2016) Anti-bacterial properties of ultrafiltration membrane modified by graphene oxide with nano-silver particles. J Colloid Interf Sci 484:107-115. https://doi.org/10.1016/j.jcis.2016.08.063
25. Tizchang A, Jafarzadeh Y, Yegani R, Khakpour S (2019) The effects of pristine and silanized nanodiamond on the performance

of polysulfone membranes for wastewater treatment by MBR system. J Environm Chem Eng 7 (6):103447. https://doi.org/10.1016/j.jece.2019.103447
26. Ali FAA, Alam J, Shukla AK, Alhoshan M, Ansari MA, Al-Masry WA, Rehman S, Alam M (2019) Evaluation of antibacterial and antifouling properties of silver-loaded GO polysulfone nanocomposite membrane against Escherichia coli, Staphylococcus aureus, and BSA protein. React Fun Poly 140:136-147. https://doi.org/10.1016/j.reactfunctpolym.2019.04.019
27. Xu Z, Ye S, Zhang G, Li W, Gao C, Shen C, Meng Q (2016) Antimicrobial polysulfone blended ultrafiltration membranes prepared with Ag/Cu2O hybrid nanowires. J Membr Sci 509:83-93. https://doi.org/10.1016/j.memsci.2016.02.035
28. de Faria AF, Martinez DST, Meira SMM, de Moraes ACM, Brandelli A, Filho AGS, Alves OL (2014) Anti-adhesion and antibacterial activity of silver nanoparticles supported on graphene oxide sheets. Colloids Surf B Biointerfaces 113:115-124. https://doi.org/10.1016/j.colsurfb.2013.08.006
29. Ireland KC, Khan A, MacLellan SR, Saha GC, Afzal MT (2024) Design, manufacturing and functionality testing of a green electrospun nanocomposite membrane for mechanical and antibacterial characteristics. Next Nanotechnol 6:100086. https://doi.org/10.1016/j.nxnano.2024.100086
30. Anekthirakun P, Imyim A (2019) Separation of silver ions and silver nanoparticles by silica based-solid phase extraction prior to ICP-OES determination. Microchem. J. 145:470-475. https://doi.org/10.1016/j.microc.2018.11.008
31. Kivi MA, Alinia H, Jafarzadeh Y, Yegani R (2019) High-density polyethylene membranes embedded with carboxylated and polyethylene glycol-grafted nanodiamond to be used in membrane bioreactors. J App Poly Sci 136:47914. https://doi.org/10.1002/app.47914
32. Khosroshahi MM, Jafarzadeh Y, Nasiri M, Khayet M (2023) Novel polyvinyl chloride ultrafiltration membranes blended with amphiphilic polyethylene glycol-block-poly(1, 2-dichloroethylene) copolymer for oily wastewater treatment. J Water Proc Eng 56:104433. https://doi.org/10.1016/j.jwpe.2023.104433
33. Reshma RP, Abishek NS, Gopalakrishna KN (2024) Synthesis and characterization of graphene oxide, tin oxide, and reduced graphene oxide-tin oxide nanocomposites. Inorg Chem Commun 165:112451. https://doi.org/10.1016/j.inoche.2024.112451
34. Widakdo J, Wu PW, Austria HFM, Hung WS, Yu PJ, Wang CF, Hu CC, Lee KR, Lai JY (2022) Dual functional GO-Ag incorporated nanocomposite pervaporation membrane with alcohol dehydration performance and enhanced antibacterial property. Mat Today Chem 24:100985. https://doi.org/10.1016/j.mtchem.2022.100985
35. Junejo Y, Safdar M, Akhtar MA, Saravanan M, Anwar H, Babar M, Bibi R, Pervez MT, Hussain T, Babar ME (2019) Synthesis of Tobramycin Stabilized Silver Nanoparticles and Its Catalytic and Antibacterial Activity Against Pathogenic Bacteria. J Inorg Organomet Polym Mater 29 (1):111-120. https://doi.org/10.1007/s10904-018-0971-z
36. Nassar MY, Shaker FA, El-Sayed GO, Masoud EM, Adam MSS, Khalil A, Rashed NM, Abdelaziz G, El-Feky HH (2024) Synthesis and characterization of lemon leaf extract-mediated silver nanoparticles: An environmentally friendly approach with enhanced antibacterial efficacy. J Mol Struct 1315:138753. https://doi.org/10.1016/j.molstruc.2024.138753
37. Chandraker K, Nagwanshi R, Jadhav S, Ghosh KK, Satnami ML (2017) Antibacterial properties of amino acid functionalized silver nanoparticles decorated on graphene oxide sheets. Spectrochim Acta Part A: Molecul. Biomolecul. Spectrosco. 181:47-54. https://doi.org/10.1016/j.saa.2017.03.032
38. Isawi H (2023) Synthesis of graphene oxide-silver (GO-Ag) nanocomposite TFC RO membrane to enhance morphology and separation performances for groundwater desalination, (case study Marsa Alam area- Red Sea). Chem Eng Proc – Proc Intensific 187:109343. https://doi.org/10.1016/j.cep.2023.109343
39. Lee J, Chae HR, Won YJ, Lee K, Lee CH, Lee HH, Kim IC, Lee JM (2013) Graphene oxide nanoplatelets composite membrane with hydrophilic and antifouling properties for wastewater treatment. J Membr Sci 448:223-230. https://doi.org/10.1016/j.memsci.2013.08.017
40. Ilyas H, Haleem A, Iqbal M, Siddiq M (2021) Influence of GO-Ag nano-filler on the antibacterial, antifouling and hydrophilic characteristics of polyvinyl chloride membrane. J Water Proc Eng 44:102336. https://doi.org/10.1016/j.jwpe.2021.102336
41. Sudapalli AM, Shimpi NG (2023) Ag@rGO coral reef morphology exhibits excellent optical properties and photocatalytic activity against methyl orange under sunlight. Diamond Relat Materi 139:110356. https://doi.org/10.1016/j.diamond.2023.110356
42. Kumar L, Mohan L, Anand R, Bharadvaja N (2024) Chlorella minutissima-assisted silver nanoparticles synthesis and evaluation of its antibacterial activity. Sys Microbio Biomanufact 4:230-239. https://doi.org/10.1007/s43393-023-00173-4
43. Al-Rawajfeh AE, Alrawashdeh AI, Etiwi MT, Alnawaiseh A, Shahid MK, Masad MHM, Oran SO, Alshahateet SF (2024) Silver nanoparticles (Ag-NPs) embedded in zeolite framework: A comprehensive study on bromide removal from water, including characterization, antibacterial properties, and adsorption mechanisms. Desali Water Treatm 317:100139. https://doi.org/10.1016/j.dwt.2024.100139
44. Pan YX, Xu QH, Xiao HM, Li CY (2023) Insights into the antibacterial activity and antibacterial mechanism of silver modified fullerene towards Staphylococcus aureus by multiple spectrometric examinations. Chemosphere 342:140136. https://doi.org/10.1016/j.chemosphere.2023.140136
45. Dridi D, Vu NN, Singh J, Eesaee M, Saidi A, Elkoun S, Nguyen-Tri P (2024) Recent advances on engineering of silver related nanocomposites toward antibacterial applications. Nano-Struct Nano-Obj 38:101195. https://doi.org/10.1016/j.nanoso.2024.101195
46. Danai L, Rolband LA, Perdomo VA, Skelly E, Kim T, Afonin KA (2023) Optical, Structural and Antibacterial Properties of Silver Nanoparticles and DNA-Templated Silver Nanoclusters. Nanomedicine 18 (9):769-782. https://doi.org/10.2217/nnm-2023-0082
47. Sun M, Li J (2018) Graphene oxide membranes: Functional structures, preparation and environmental applications. Nano Today 20:121-137. https://doi.org/10.1016/j.nantod.2018.04.007
48. Kazerouni HN, Jafarzadeh Y, Yegani R (2020) Study on the

effect of m-phenylenediamine as a cross-linking agent on the mechanical, chemical and thermal properties and performance of cellulose acetate/nanodiamond membranes. Polymer Bulletin 77:405-425. https://doi.org/10.1007/s00289-019-02758-3

49. Jiang Y, Zeng Q, Biswas P, Fortner JD (2019) Graphene oxides as nanofillers in polysulfone ultrafiltration membranes: Shape matters. J Membr Sci 581:453-461. https://doi.org/10.1016/j.memsci.2019.03.056
50. Nam NTH, Dat NM, An TTV, Tinh NT, Phuc TCV, Huong LM, Hai ND, An H, Cong CQ, Tai LT, Chau PTL, Oanh HN, Khoa TD, Hieu NH (2024) Insight biological prospects of silver@graphene oxide nanocomposite synthesized by Muntingia calabura leaf extract: Stunning ROS-related antibacterial mechanism under visible light. J Drug Deliv Sci Technol 93:105459. https://doi.org/10.1016/j.jddst.2024.105459
51. Mukherjee K, Bhagat N, Kumari M, Choudhury AR, Sarkar B, Ghosh BD (2023) Insight study on synthesis and antibacterial mechanism of silver nanoparticles prepared from indigenous plant source of Jharkhand. J Genet Eng Biotechnol 21:30. https://doi.org/10.1186/s43141-023-00463-3